Proceedings of the ASME 2010 Pressure Vessels & Piping Division / K-PVP Conference
PVP2010
July 18-22, 2010, Bellevue, Washington, USA

PVP2010-25814

AN EXPERIMENTAL APPROACH FOR DELAYED STRESS CORROSION

Scott G. Keller
University of Central Florida
Orlando, Florida, USA

Ali P. Gordon
University of Central Florida
Orlando, Florida, USA

ABSTRACT

Failures of structural and mechanical components have long been attributed to environmentally assisted cracking (EAC). The umbrella of EAC encompasses several phenomena, including stress corrosion cracking (SCC), corrosion fatigue (CF), hydrogen embrittlement (HE) and liquid metal embrittlement (LME). The latter, LME, has resulted in the failure of components in petrochemical and aeronautical industries, among others. The effects are detrimental, with crack tip velocities on the order of centimeters per second and failures occurring rapidly. Previous research has provided numerous underlying microstructural failure mechanisms aimed at identifying the true failure mode. Conflicting experimental data has extended the debate over the true mechanism promoting renewed interest in novel experimental regimes. Utilizing fracture mechanics specimens, the solid-liquid Al-Hg couple was analyzed to extend or reject current theories. Through the implementation of an original environmental chamber capable of testing notched and pre-cracked components in corrosive environments, C(T) specimens were subjected to experiments submersed in liquid mercury. Upon the application of an initially applied stress intensity factor (under load-control), incubation periods preceding failure were observed. Crack initiation and propagation were observed to occur along the starter notch, as well as other regions on the specimen. Results provided evidence that additional factors, such as a critical load or critical microstructural orientation, were factors in crack initiation and propagation. In the quest to observe the influence of these additional factors, a variation of the experimental setup was implemented and initial tests have begun.

INTRODUCTION

Environmentally assisted cracking (EAC) is a widely known phenomenon that has been extensively researched throughout the 1900's [1,2]. An encompassing term, EAC includes hydrogen embrittlement (HE), corrosion fatigue (CF), stress corrosion cracking (SCC) and liquid metal embrittlement (LME). Each subset of EAC has been observed to cause failures in structural members of mechanical designs, sometimes with catastrophic results [1,2]. While some modes of EAC are not as common as others, e.g. LME as opposed to SCC or HE, the result is still the same; failure more rapidly than anticipated.

Stress corrosion cracking became a mainstream issue during the World War II era, in which several Liberty ships experienced through hull failures. It was determined that a combination of the new weld techniques coupled with the cold saltwater environment and microstructure of the hull material, cracks were able to originate and propagate, resulting in the highly publicized rupture of the hulls. Notable consideration was given to the crack velocities, as failures were described as instantaneous. During this time, fracture mechanics was developed to help explain such failures [3].

Fracture mechanics is largely based upon the development of mathematical models of Inglis and Griffith [4]. Inglis implemented the theory of elasticity to solve the problem of an elliptical hole, while Griffith used energy methods to quantify brittle fractures. Taking this theory, Irwin was able to successfully apply it to ductile materials, as well as define the stress intensity factor, *SIF* or *K* [4].

In the presence of a crack, *K* defines the stress field surrounding the defect. Under plane-strain conditions, *K* is considered a material constant. Upon reaching a critical value known as the plane-strain fracture toughness, K_{Ic}, cracks can be expected to grow and propagate. The speed at which they propagate is largely affected by the surrounding environment, making it an extremely useful tool in the study of EAC.

Studies aimed at quantifying the effects of SCC have implemented blunt notch specimens, as well as fracture mechanics pre-cracked specimens. Upon placing smooth tensile specimens in 3.5% NaCl, Gordon et al. observed crack initiation resistance was lower than that of specimens in air [5]. Similarly, by introducing specimens to a humid environment, Spiedel demonstrated the effect that moisture had on crack velocities [6]. By introducing water, crack tip velocities were observed to increase as the level or moisture in the environment increased, Fig. 1. From a completely dry environment to a

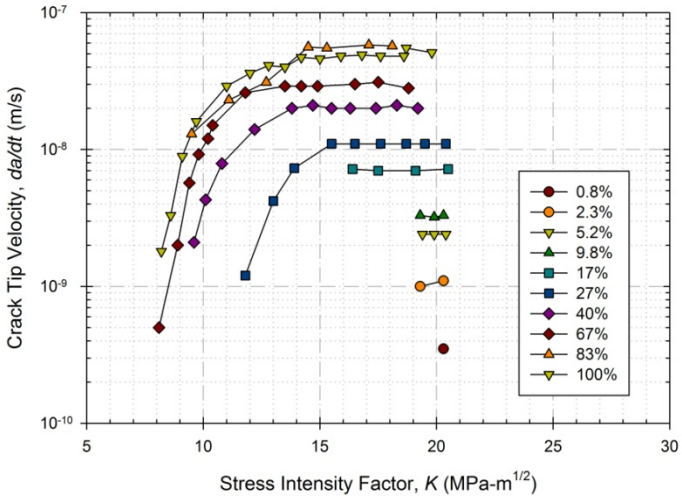

***Figure 1**: Effect of humidity on crack tip velocities, Speidel, 1975.*

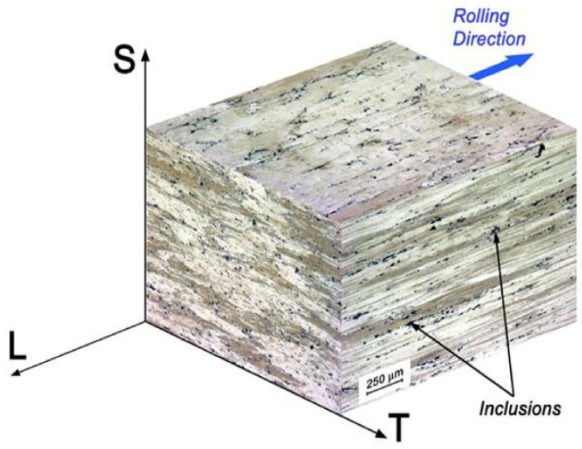

***Figure 2**: Microstructure of Al 7075-T651.*

fully humid environment, crack velocities increased nearly three orders of magnitude.

A more significant increase in crack tip velocities is observed during liquid metal embrittlement. Although occurrences are not as frequent as other modes, the severity is extreme. In 1987, an ethylene plant experienced a failure in an aluminum pipe weld due to exposure to liquid mercury [7]. It was noted that mercury does not wet aluminum well as a result of oxide formation, but in the event of corrosion, fatigue and other events, wetting can occur. Once it does, chemical and mechanical interactions occur that reduce the load carrying capabilities of the solid material.

Several researchers have studied the effect liquid metals have on the reduction of load carrying capabilities. Incubation tests were conducted by Nichols and Rostoker, as well as Gordon and An, on smooth tensile specimens [8,9]. Fatigue crack growth experiments, using fracture mechanics specimens, have been conducted, like those of Kapp et al. and Benson and Hoagland, in which crack tip velocities were seen to be on the order of centimeters per second [10,11]. The results and conclusions provided by these groups, as well as others, have assisted in defining the crack tip driving forces and underlying failure mechanisms; however, there still exists some uncertainty.

Two leading theories regarding the underlying failure mechanism are the Decohesion Model, proposed by Stoloff and Johnston, and Westwood and Kamdar, both in 1963 [12,13], and the Adsorption Induced Dislocation Emission Model, proposed by Lynch in 1977 [14].

The Decohesion Model is rooted in the energy associated with fracture. During fracture, two surfaces are created, which involves a transfer of energy to occur. This model is fundamentally rooted in the free energy relationship developed by Girffith. Through chemical interactions during LME, the energy required to generate the two surfaces decreases. A resulting reduction in the normal-to-shear strength in the bonds of the solid metal occurs, allowing for failure at a lower tensile stress. As strong of a model as it is, it does have a drawback in that it assumes no plastic deformation occurs during rupture.

The Adsorption Induced Dislocation Emission Model is based on the chemisorption of liquid metal on the solid metal surfaces. It deals with surface energies, similar to that of the Decohesion model; however, it allows for some plastic deformation during rupture. Through SEM analysis, Lynch was able to identify microvoid coalescence (MVC) with limited amounts of plasticity. Through nucleation and egression of dislocations, cracks would propagate in the solid exposed to liquid metals by shearing of interatomic bonds.

The two theories presented here are just a few of the several that have been proposed throughout the century. Two other examples are the models by Robertson, the Stress Assisted Dissolution Model and by Krishtal et al., the Grain Boundary Diffusion Model [15,16]. Each of these models have their strengths for particular couples; however, research has provided contradictory experimental data [10, 17-18].

Though these models are sufficient for some solid-liquid metal couples, not all instances can be described by these modes of failure. As stated, several groups have experimented with solid-liquid couples. The results revealed that the embrittlement of the solid metal was severe and that crack tip velocities were orders of magnitude greater than counterparts fractured in air. Although the research was conclusive, one theme was constant throughout the experiments; there was not a continuous supply of embrittler available at the crack tip, therefore LME conditions may or may not have existed for the entirety of the fracture process.

In most previous experiments, a few drops of liquid embrittler were applied to specimens. In some cases, acids, e.g. HF, were used to remove the oxide layer to achieve proper wetting. Researchers noted that oxide formation in aluminum inhibits the wetting process, thus inhibiting LME conditions [19]. Upon fracture, it was not noted if the volume of liquid embrittler was sufficient enough to wet the entire fracture surface. If at any time oxides are allowed to form due an

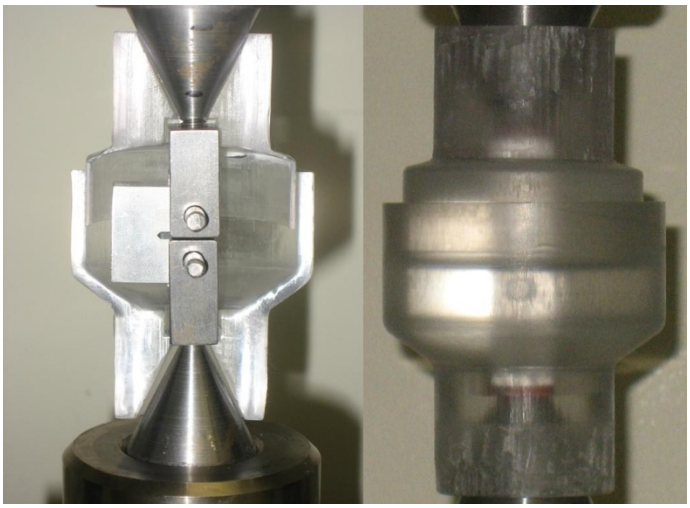

Figure 3: *(a) Cutaway view of environmental fracture bath with specimen loaded and (b) View of environmental fracture bath with specimen loaded and submersed.*

insufficient amounts of embrittler, true LME conditions would not be achieved.

Additionally, stress intensity factors well below the established K_{Ic} were observed to cause rupture in specimens. Stress intensity factor ranges were used in testing; however, the influence of a static *SIF* has on a specimen was loosely studied. In most cases, the *SIF* was merely recorded and was not a primary variable used to control these experiments. Threshold values of K_I have been investigated, leading to a notion of a K_{ILME} in which if

$$K_I < K_{ILME},$$

no failure will occur. Static incubation tests, conducted at varying stress intensity levels, will further define this threshold value.

The two concerns mentioned, an insufficient amount of liquid embrittler and the influence of a static *SIF*, have the possibility of significantly altering the affect liquid metals have on solid, structural metals. New experimental procedures are required to fully understand how structural materials will behave in the presence of liquid metals.

EXPERIMENTAL METHOD

During the course of this research, two novel methods of subjecting fracture specimens to a continuous supply of liquid metal were developed. The first set of experiments involved traditional C(T) fracture specimens that were loaded into a specially designed environmental bath capable of loading specimens while fully submersed in a liquid metal. More recently, a new method involving four point bend experiments is being implemented to compare the results and provide new insight on the crack initiation process.

The solid material chosen for this study is the peak-aged aluminum alloy Al 7075-T651. This particular alloy contains a large amount of Zinc and Magnesium, as well as 10μm inclusions, typically $MgZn_2$. The grains are pancake-like, with a representative microstructure shown in Fig. 2. The

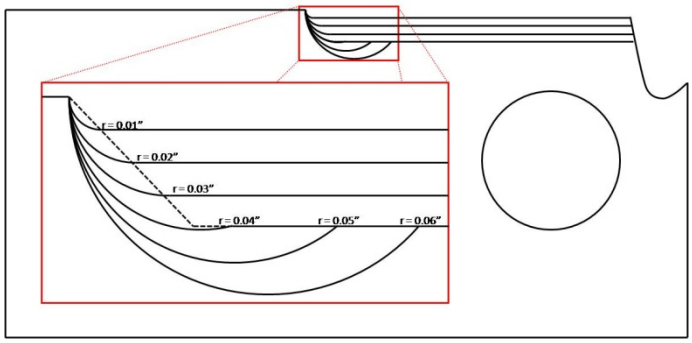

Figure 4*: Blunt notch C(T) specimen (half) with various notch root radii prior to fatigue pre-cracking.*

orientation of the C(T) specimen is S-L, allowing for the crack to propagate in the rolling direction of the sheet. This particular orientation provides a uniform microstructure ahead of the crack trip, eliminating effects due to the cold working process. As Al 7075 is a commonly used structural material, it has been observed to be extremely susceptible to LME, as well as SCC, making it a suitable candidate to use during the experimental portion of this study.

The metal that was selected to serve as the liquid embrittler was mercury (Hg). As Hg is a liquid at room temperature, it is an ideal liquid to be used at room temperature experiments in an environmental bath. Additionally, mercury does not readily penetrate grain boundaries, as the solubility parameter difference between aluminum and mercury is high. Coupled with the lack of easily "wetting" surfaces, mercury was chosen to serve as the embrittling metal.

The environmental fracture bath was designed to work with conventional C(T) fracture specimens loaded under uniaxial tension. Additions to the bath can incorporate a clip gage and heating elements to expand the solid-liquid couples past those that include metals liquid at room temperature. A cutaway view of the chamber is given, Fig. 3a, as well as a view of the chamber loaded with a specimen and liquid, Fig. 3b. The result is a chamber capable of submersing a C(T) specimen while applying mechanical loads.

In addition to the environmental fracture bath, a modified four-point bend experiment was developed to test both conventional C(T) fracture specimens, as well as blunt notch specimens, Fig. 4. The setup involved attaching two rigid arms to the top and bottom of a C(T) specimen, effectively creating a C(B) specimen, Fig. 5. Several advantages are provided by adding these arms as opposed to using standard bend specimens, as it necessitates the use of only one geometry capable of being implemented in a variety of experimental setups. Additionally, it reduces the amount of material required to test specimens oriented in the S-L orientation. In conventional bend experiments, rolled sheets with large thicknesses (several inches) would be required. With this set up, small samples can be utilized, reducing material and machining costs.

To subject the C(B) fracture or blunt notch specimens to a liquid environment in the four point bend experiments, a

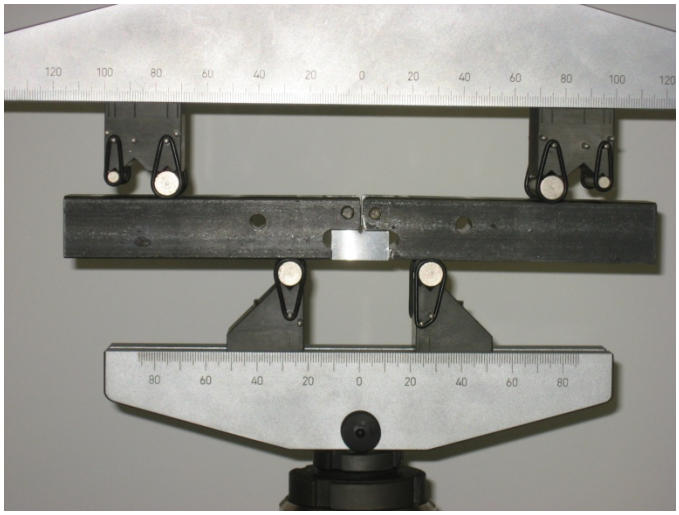

Figure 5*: Rigid arms attached to C(T) specimen to be used in four point bending.*

Figure 6*: Specimen coated with heat shrink providing envelope for liquid metal.*

polymer was used to surround the specimen. Polyolefin, more commonly known as shrink wrap, was used to conform to the specimen, Fig. 6. The design incorporates voids along the side of the specimen to allow for mercury to be readily available upon any crack initiation and growth.

Experiments were conducted on a servohydraulic MTS 100kN load frame with the Teststar IIs control station in accordance with ASTM E399, the experimental standard for plane strain fracture toughness testing. During the fatigue pre-cracking portion, a tension-tension load ratio, *R*, of 0.1 was used at a rate of 1 Hz. Upon reaching a suitable crack length, as defined by E399, the pre-cracking regime concluded. Subsequent tests, either a plane strain fracture test or an incubation at an initial *SIF* test, was conducted, without removing the specimen from the bath. This is key, as removing the specimen from the bath could induce oxide formation, thus inhibiting the wetting necessary for LME conditions.

Monitoring the application of load and crack mouth opening displacement, *CMOD*, was conducted in two different fashions, depending on the experimental setup chosen. The environmental fracture bath measured load via the load cell attached to the load frame while the *CMOD* had to be approximated through the load frame displacement. The relationship between *CMOD* and crosshead displacement is highly linear and provided an accurate approximation of the *CMOD* in real time. During the four point bending, load was monitored via the load cell, while a clip gage was incorporated to directly measure the *CMOD*, allowing for the real time approximation of the crack length, Fig. 7. During incubation experiments, real-time crack lengths can be monitored up until the time to failure, Fig. 8.

Upon the completion of pre-cracking, in the case of C(T) fracture specimens, incubation or plane strain fracture tests were conducted. Plane strain fracture tests were conducted under load control per E399 guidelines. Incubation experiments involved loading the specimen to an approximated initial *SIF* and allowed to remain loaded until fracture occurred, thus observing the time to rupture. In experiments involving blunt notch specimens, a load was applied and allowed to incubate until crack advancement was noted through a change in the *CMOD*.

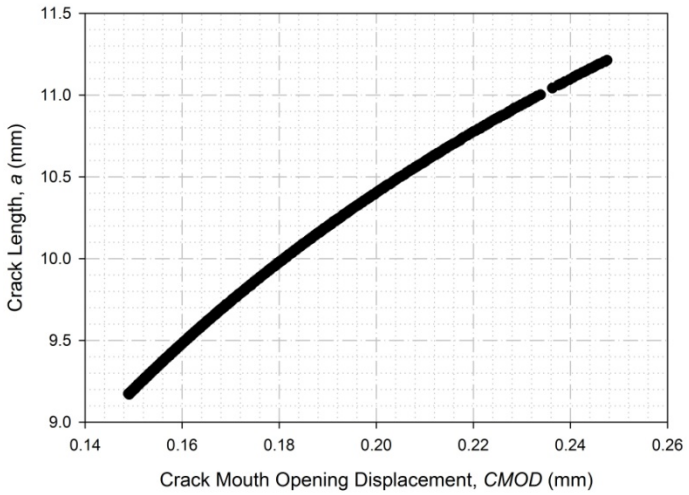

Figure 7*: Real-time approximation of the crack length via CMOD.*

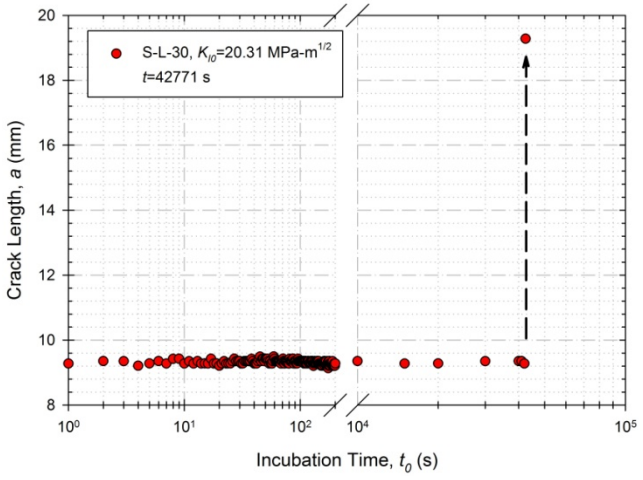

Figure 8*: Crack length measured during incubation experiment, in which rupture occurred in less than 0.1 seconds.*

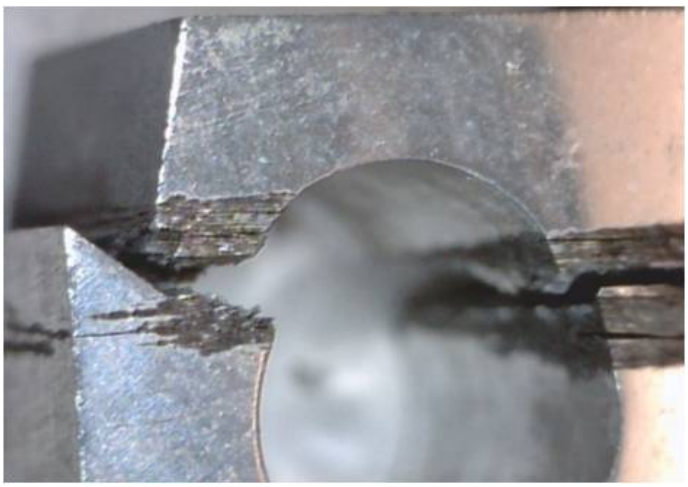

Figure 9*: Rupture of specimen with crack initiation in the load pin hole.*

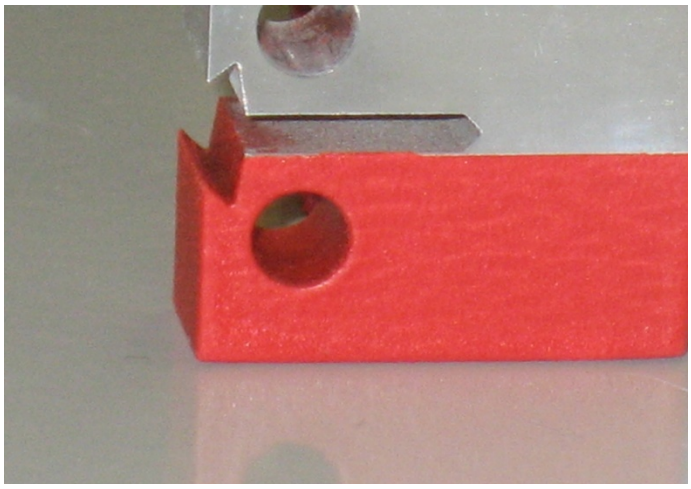

Figure 10*: Rubberized coating applied to the lower half of C(T) specimens tested in the environmental fracture bath.*

Upon rupture, specimens were removed from the load frame, taking care to preserve the fracture surface. Specimens were subsequently viewed under magnification to measure crack length and to calculate the value of *K*. Inspecting the load-displacement graphs subsequently allowed for the determination of the validity of the experiment and if *K* was the critical value, K_{Ic}. If the specimen met the requirements of E399, it was counted and used in reporting the results.

Additional analyses were conducted at the University of Central Florida's Materials Characterization Facility. Ruptured specimens were viewed under a SEM and underwent EDX analyses. The EDX was used to ensure that the liquid embrittler was observed at all points on the surface, while the images obtained were to be used in characterizing the mode of fracture.

RESULTS AND DISCUSSION

Base-line experiments were conducted in standard laboratory conditions, i.e. room temperature with approximately 50% humidity, to use in comparisons between air and liquid environments. Experiments were additionally conducted in 3.5% NaCl. Saltwater is known to cause SCC in Al 7075, therefore a drop in the K_{Ic} was expected. The values obtained in air and saltwater were 25.6 MPa·m$^{1/2}$ (23.5 ksi·in$^{1/2}$) and 23.1 MPa·m$^{1/2}$ (21.2 ksi·in$^{1/2}$), respectively, which demonstrates the effect environment has on the fracture resistance of a material.

Utilizing liquid mercury as the working fluid, the rupture of specimens was observed at several locations, including along the knife edge, the knife edge valley and the load pin hole, Fig. 9. The mercury attack was severe enough to result in crack initiation at locations of a critical stress build up and not necessarily at the location of a stress intensity due to a crack. These issues were not previously reported by other research groups, as the embrittling metal was only applied to the machined notch/pre-crack and not the entire specimen. In order to channel crack initiation at the starter notch/pre-crack, the bottom half of specimens were coated with a rubberized coating and the knife edge valley was filleted on subsequent specimens that were ordered, Fig. 10.

After implementing the coated specimens, rupture was occurring solely at the pre-crack. The fracture surfaces were notably different than those fractured in air and saltwater environments. Several crack initiation sites were observed along the knife edge, as well as severe discoloring of the surface, Fig. 11. Under plane strain conditions, the average value of K_{Ic} was 24.9 MPa·m$^{1/2}$ (22.7 ksi·in$^{1/2}$).

In studying the incubation points, specimens were pre-cracked in liquid mercury, the load was removed and then loaded to an estimated *K* under load control. Ultimately, a *K* versus failure time graph is generated, similar to that of a S-N plot used in fatigue, Fig. 12. Scatter in the data points is apparent, similar to the scatter observed in reporting fatigue life data. Approximately 35 experiments have been conducted in various environments and routines with more planned to provide more results on the dependency of the applied *SIF* and failure time.

In Fig. 12, several regions are highlighted, as to the expected regimes that exist during the incubation process. Some specimens were observed to fail instantaneously as the load was applied. Failures were observed to occur on the order of a few seconds. It is proposed that failure occurs as a result of multiple crack initiation locations along the starter notch, providing several cracks to coalesce and propagate. The stress fields by the presence of each crack overlap, creating a more complex state of stress, which leads to instantaneous rupture.

Specimens that incubated for an extended period of time are proposed to go through a region where possible time-dependent diffusion can occur, dependent upon the couple. For the Al-Hg couple, this is unexpected, as the solubility parameter difference is high; however for couples that have a lower difference, this will have an effect on the time to failure. Upon concluding the time-dependent incubation regime, specimens enter a region of stable crack growth.

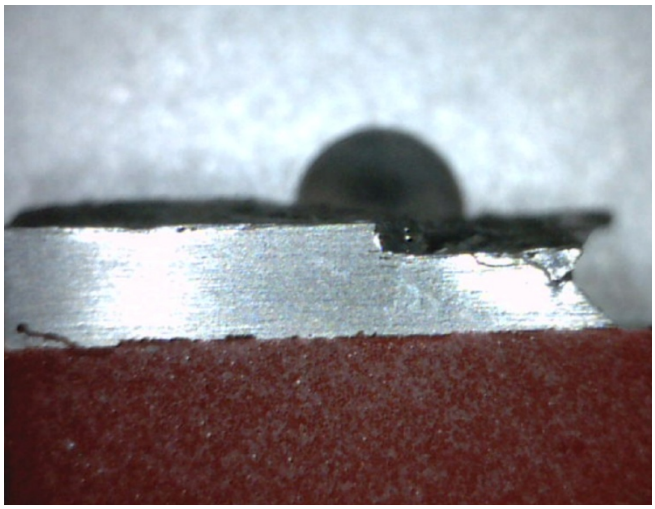

Figure 11*: Multiple crack initiation locations, as well as transgranular cracking.*

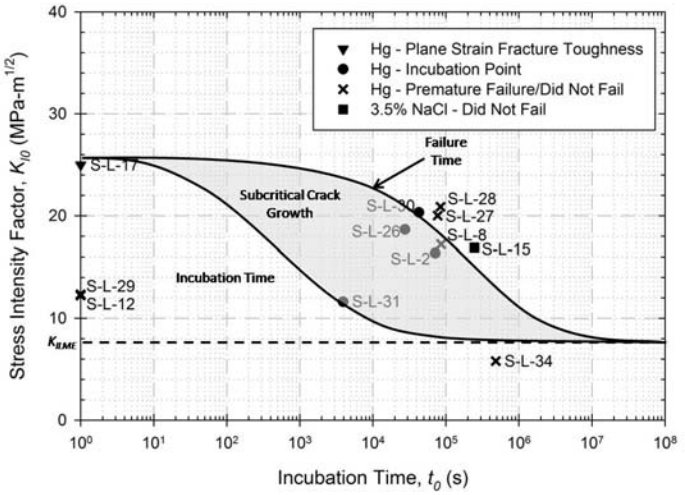

Figure 12*: Stress Intensity Fracture versus Incubation/Rupture Time plot.*

Depending on the specimens used, this stable crack growth regime could be nonexistent, as was the case in these experiments. Any advancement in the crack tip resulted in complete rupture of the specimens. Crack velocities were observed to be consistent with previous results and on the order of centimeters per second.

Similarly to an S-N curve, the rupture line dictates the two regimes where fracture is either expected or not. To more clearly define this line, several more experiments are necessary. Fatigue curves display similar scatter in results, clearly indentifying that more points are necessary to narrow down the rupture line.

An additional observation was made regarding the specimens that failed to rupture after a predetermined amount of time that was based on the initially applied *SIF*. These specimens could have been subjected to oxidation through re-used mercury, among other processes that inhibited LME conditions. Since, the reuse of mercury has been limited to only a few specimens, ensuring that oxide content with in the mercury is low.

Fractured specimens were subsequently viewed under SEM and EDX analyses were conducted. The SEM provided valuable information regarding the mode of fracture. Several specimens fractured in liquid mercury had regions of transgranular-like cracking and extensive secondary cracking, Fig. 13. After extensive searching, several regions of dimples were observed, indicating that limited amounts of plastic deformation occurred during rupture, Fig. 14. The significance of plastic deformation is that it supports the AIDE failure model.

EDX analyses conducted on the fractured surface provided evidence that mercury had completely covered the surface. Adsorption occurred during the fracture process, again supporting the AIDE model. The environmental chamber successfully displayed it was able to supply a sufficient amount of embrittler; a key issue that was missing in previous reports.

The results from experimentation with the environmental fracture bath led to the development of the second test method. The most compelling evidence deals with the specimens that failed instantaneously upon the application of load. It was noted that either a critical load or microstructural orientation would lead to crack initiation and subsequent rupture. With several sites for crack initiation to occur, the four point bend apparatus is to be implemented.

Using blunt notch C(T) specimens with varying root radii, the effect of a critical stress concentration is currently under investigation. Additionally, orienting the blunt notch specimens in various orientations, e.g. T-L, L-T, etc., will provide insight as to any microstructural orientation-based dependency. Essentially, the stress concentration provided by the root radius will provide a clearly defined stress at the root. Crack initiation is monitored through *CMOD*, and once initiation is observed, specimens are fractured and removed from the apparatus.

Experiments involving four point bending are currently ongoing. Early predictions establish a critical stress as a defining parameter for crack initiation for this particular solid-liquid couple. Several other couples are to be explored to determine the validity over a wide variety of solid-liquid couples and more precisely determine the underlying failure mechanisms of LME.

CONCLUSIONS

As mechanical designs evolve and progress, new designs will be subjected to a variety of environmental conditions. The interaction between the design and its surrounding environment will undoubtedly come into concern. Understanding the fatigue and fracture of materials within these environments will significantly aid designers in the material selection process. Through the implementation of two novel experimental routines, the affect liquid environments, namely liquid metals in this study, have on the fracture of structural materials are observed. There exists a delicate balance between the applied load, stress concentrations and the microstructural orientation

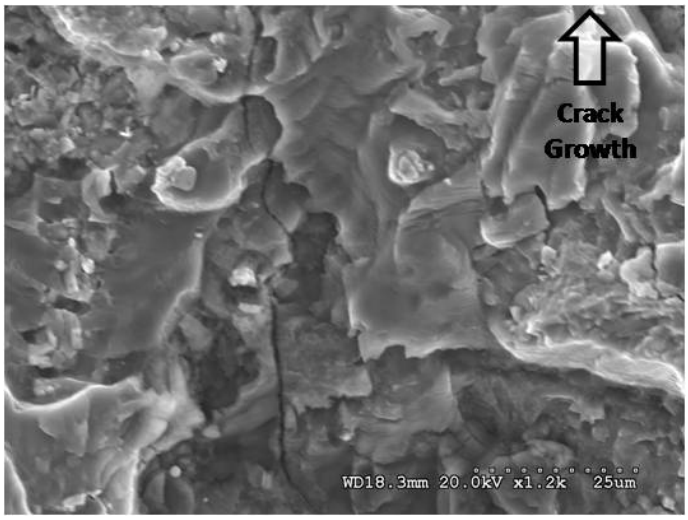

***Figure 13**: SEM image of a fracture surface, with extensive secondary cracking, fractured in Hg environment.*

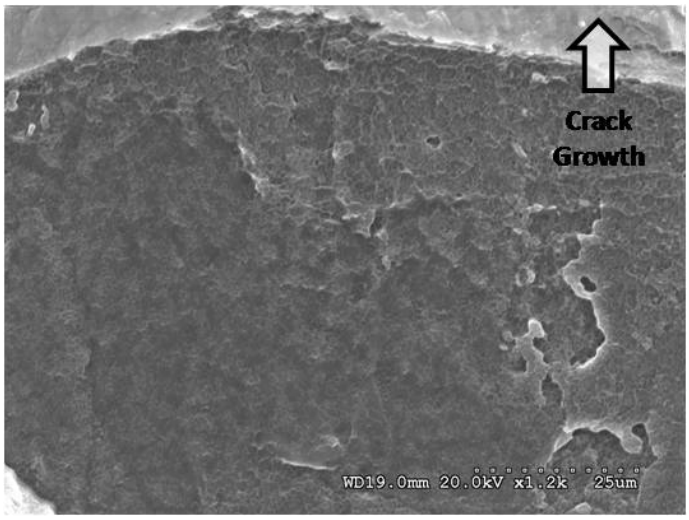

***Figure 14**: Small region in which ductile dimples were observed, providing evidence of localized plastic deformation (fractured in Hg environment).*

that will dictate failure. By utilizing the experimental methods outlined, a wide variety of solid-liquid couples can be explored. The result will be a better understanding of the susceptibility to EAC and the failure mechanisms that drive the crack tip.

REFERENCES

[1] Lynch, S.P., *Failures of Structures and Components by Environmentally Assisted Cracking*, Engineering Failure Analysis, Volume 1 (2), pp. 77-90, 1994.

[2] Lynch, S.P., *Failures of Engineering Components Due to Environmentally Assisted Cracking*, Practical Failure Analysis, Volume 3 (5), pp. 33-42, 2003.

[3] Sumpter, J.D.G., and Kent, J.S., *Prediction of Ship Brittle Fracture Casualty Rates by a Probabilistic Method*, Journal of Marine Structures, Volume 17 (8), pp. 575-589, 2004.

[4] Sanford, R.J., *Principles of Fracture Mechanics*, Upper Saddle River, NJ: Pearson Education Inc., 2003.

[5] Gordon, D.E., et al., *Effects of Salt Water Environment and Loading Frequency on Crack Initiation in 7075-T651 Aluminum Alloy and Ti-6Al-4V*, Corrosion Cracking Conference, ASM International, pp. 157-165, 1986.

[6] Speidel, M., *Stress Corrosion Cracking of Aluminum Alloys*, Metallurgical Transactions A, Volume 6 A (4), pp. 631-651, 1975.

[7] English, J.J. and Korbin, G., *Liquid Mercury Embrittlement of Aluminum*, Materials Performance, Volume 28 (2), pp. 62-63, 1989.

[8] Nichols, H. and Rostoker, W., *On the Mechanism of Crack Initiation in Embrittlement by Liquid Metals*, Acta Metallurgica, Volume 9 (5), pp. 504-509, 1961.

[9] Gordon, P. and An, H., *The Mechanisms of Crack initiation and Crack Propagation in Metal-Induced Embrittlement of Metals*, Metallurgical Transactions A, Volume 13A, pp. 457-472, 1982.

[10] Kapp, J., et al., *Crack Growth Behavior of Aluminum Alloys Tested in Liquid Mercury*, Journal of Engineering Materials and Technology, Volume 108 (1), pp. 37-43, 1986.

[11] Benson, B.A. and Hoagland, R.G., *Crack Growth Behavior of a High Strength Aluminum Alloy during LME by Gallium*, Scripta Metallurgica, Volume 23 (11), pp. 1943-1948, 1989.

[12] Stoloff, N.S. and Johnston, T.L., *Crack Propagation in a Liquid Metal* Environment, Acta Metallurgica, Volume 11 (4), pp. 251-256, 1963.

[13] Westwood, A.R.C and Kamdar, M.H., *Concerning Liquid Metal Embrittlement, particularly of Zinc Monocrystals by Mercury*, Philosophical Magazine, Volume 8 (89), pp. 787-804, 1963.

[14] Lynch, S.P., *Effect of Environment on Fracture – Mechanisms of Liquid Metal Embrittlement, Stress-Corrosion Cracking and Corrosion-Fatigue*, International Conference on Fracture 4, Pergamon Press, Volume 2, pp. 859-866, 1977.

[15] Robertson, W.M., *Propagation of a Crack Filled with Liquid Metal*, Metallurgical Society of American Institute of Mining, Metallurgical and Petroleum Engineers – Transactions, Volume 236 (10), pp. 1478-1482, 1966.

[16] Krishtal, M.A., et al., *Diffusion of Impurity Atoms along Dislocations in Aluminum*, Physics of Metals and Metallography, Volume 36 (5), pp. 191-193, 1973.

[17] Wheeler, D.A., *Stable Crack Growth during the Liquid Metal Embrittlement of Aluminum by Mercury*, PhD Dissertation, The Ohio State University, 1987.

[18] Wanhill, R.J.H., *Cleavage of Aluminum Alloys in Liquid Mercury*, Journal of Corrosion Science and Engineering, Volume 30 (10), pp. 371-378, 1974.
[19] Wheeler, D.A., et al., *Evidence for Crack Tip Oxidation Effects During the Liquid Metal Embrittlement of AA 7075 Aluminum Alloy by Mercury*, Corrosion, Volume 45 (3), pp. 207-212, 1989.